

Improving 5G uplink spectral efficiency using massive multiple-input multiple output and non-orthogonal multiple access

Enebe, C. C.^{1.}, Agwu, E. O.^{2.}, Nnebe, U. S.³ and Idigo, V. E.⁴

^{1&2}Michael Okpara University of Agriculture. Umudike.

^{3&4}Nnamdi Azikiwe University, Awka.

*Corresponding Author's E-mail: agwu.ekwe@mouau.edu.ng and enebe.canice@mouau.edu.ng

Abstract

This paper investigates the integration of massive multiple input multiple output (MIMO) architecture with non-orthogonal multiple access (NOMA) technology. The primary objective is to address the growing demand for higher data rates by extending communication frequencies into the millimeter wave (mmWave) band while simultaneously enhancing system spectral efficiency in the uplink (UL). The uplink (UL) operation of massive MIMO–NOMA was considered, where the base station (BS) is equipped with massive antenna array that uses hybrid precoding of Zero Forcing (ZF), Maximum Ratio Transmit (MRT) and Minimum Mean Square Error (MMSE) to reduce the number of required radio-frequency (RF) chains without performance loss, less hardware cost and Signal Interference Cancellation to mitigate against far and near problem. A comprehensive system model and mathematical framework for massive MIMO–NOMA are developed and implemented using MATLAB software. The power coefficient and fading factor was generated using Monte Carlo simulation. It was observed that at the UL, the issue of user performance relative to their proximity to the base station is effectively addressed. However, the weakest user (user1) outperforms the strongest user (user10) at transmitting power of 20dBm by 18%. Other findings reveal that User6 and user8 outperform user10 by 45% in terms of best capacity, even when user10 is physically closer to the base station. These results were obtained using QPSK modulation. In summary, combining massive MIMO and NOMA holds great potential for improving uplink (UL) performance, particularly in millimeter-wave (mmWave) communication scenarios.

Keywords: Massive Multiple Input Multiple Output, Non-orthogonal Multiple Access, Zero Forcing, Maximum Ratio Transmit, Minimum Mean Square Error

1. Introduction

To meet the ever increasing demand in data rate, Non-Orthogonal multiple access (NOMA) technology has been adopted and Integrating with Massive Multiple Input Multiple Output (MIMO) architecture, (Shiguo *et.al.*, 2021). Massive MIMO–NOMA is a hybrid technology that overcomes a myriad of problems in the 5G cellular system and beyond, including massive connectivity, low latency, and high dependability, (Mohamed *et.al.*, 2022). This paper aims to enhance the spectral efficiency of fifth-generation (5G) networks using Massive MIMO–NOMA techniques. Massive MIMO–NOMA combines the spatial multiplexing capabilities of massive MIMO with the power domain sharing of NOMA. According to (Hieu, 2020), the rapid growth in massive connectivity, driven by billions of devices connected to dense networks such as the Internet of Things (IoT), underscores the need for innovative technologies to ensure Quality-of-Experience (QoE). Recently, many novel approaches have been introduced as potential solutions for future wireless networks, (Antonio *et.al.*, 2024). In massive MIMO systems, tens or hundreds of Base Station (BS) antennas transmit data to hundreds or thousands of users, each equipped with a single or multiple antennas (David *et.al.*, 2022). The technology is seen to scale-up the data rate by instantaneously transferring the data within a limited bandwidth. The technology is characterized by important features such as huge degrees of freedom, lower consumption of transmission power, higher spectral efficiency, and reliability, (Tasher *et.al.*, 2019). Notably, Massive MIMO–NOMA has been shown to support Multiple Access (MA) efficiently,

especially when the number of antennas at the BS exceeds the number of User Equipment (UEs) (Senel *et.al.*, 2019). Two main technologies have been considered to improve the spectral efficiency of 5G networks: Non-orthogonal Multiple Access (NOMA) and massive Multiple-Input Multiple-Output (mMIMO).

Non-Orthogonal Multiple Access (NOMA) allows multiple UEs to efficiently share the same time-frequency resources. This approach enhances throughput and rate fairness, even when the ratio of antennas to UEs is limited (Linglong *et.al.*, 2018). This paper studied the performance of NOMA, for both conventional and cooperative NOMA, associated to mMIMO. Advances in technologies and the rise of new applications, such as unmanned vehicles, smart homes, smart grid, and massive sensor networks, are triggering an accelerated growth in the number of devices connected to communication systems. In response to the rapid growth in wireless communication demands, the development of the fifth generation (5G) of networks is well underway. These 5G systems have already been deployed globally, marking a significant milestone. As we look beyond 5G, networks are expected to meet a diverse set of requirements, ranging from massive connectivity and ultra-low latency to enhanced user fairness. The evolution of wireless technology continues to shape our connected world. MIMO is being credited as one of the key enabling components of 5G, (Arthur, *et.al.*, 2020). Specifically, by deploying an extensive array of antennas and leveraging spatial multiplexing, massive MIMO technology holds the promise of reducing system latency and delivering significant connectivity improvements., (Albreem *et.al.*, 2021), (Elhefnawy *et.al.*, 2022).

Power-domain NOMA is another promising technology for the future-generation wireless systems that allow multiple users to be served in parallel within the same frequency and time slot, (Mohamed *et.al.*, 2023). The relying concept of NOMA consists of superposing the data symbols of different users in the power domain at the BS and employing Successive Interference Cancellation (SIC) at the receivers, (Robin *et.al.*, 2020), (Albreem *et.al.*, 2020), with such features, NOMA can also provide massive connectivity capabilities and a reduction in latency to the network. If the NOMA technique is applied to massive MIMO, the achievable spectral and connectivity improvements are shown to be even greater. Two main technologies have been considered to improve the spectral efficiency of 5G networks: non-orthogonal multiple access (NOMA) and massive multiple-input multiple output (mMIMO). A system that combines m-MIMO with NOMA, results in an efficient use of the available spectrum, while keeping the interferences at a low level, and therefore, improving the performance of the system, (Mário *et.al.*, 2021), (Samarendra *et.al.*, 2022).

To meet the ever-increasing high demand in data rate, massive MIMO-NOMA transceiver are considered for 5G and beyond wireless communications systems. To decrease hardware cost and power consumption without rendering significant spectral efficiency loss, hybrid precoding were used in massive MIMO systems (Shiguo *et.al.*, 2021), in this paper Zero Forcing (ZF), Maximum Ratio Transmission (MRT) and Minimum Mean Square Error (MMSE) precoding was combined to achieve a hybrid precoding for massive MIMO. On the other hand, to improve system spectral efficiency through the spectrum sharing concept, NOMA technology has been adopted, and the proposed system model showing power domain superposition at the transmitter side and implementation of Successive Interference Cancellation (SIC) for different distances for the ten users at the receiver side. The two technologies (massive MIMO and NOMA) were combined to improve the data rate and spectral efficiency of 5G network to meet the high demand for data rate for Internet of Things (IoT), Device to Device connection (D2D), Machine to Machine (M2M) and vehicle to everything (V2X) connection etc, without altering the available bandwidth or increasing the transmit power of the network.

In this paper, the system model for massive MIMO-NOMA network and mathematical model for the uplink of the massive MIMO-NOMA network was developed. The models demonstrated the massive connectivity ability of massive MIMO-NOMA with ten users while previous authors like (Chen *et al.*, 2018), (Hieu V *et al.*, 2020), (Dang *et al.*, 2022) (Ridho *et al.*, 2023), (Linglong *et al.*, 2018) only used two users, showing just the near user and far user except (Mohamed *et.al.*, 2023) that used four users only and failed to show how the problem of far and near can be totally eliminated by deployment of massive MIMO-NOMA scheme without increasing the bandwidth and the transmitting power of the already existing 5G network and equally failed to state the hybrid precoding technique used or show the performance of the network in terms of spectrum efficiency at the UL. (Mohamed *et.al.*, 2023) also achieved optimal result with 200MHz bandwidth while the testbed bandwidth used in this work to achieved optimal result is 100MHz.

2.0 Material and methods

2.1 System Model for Massive MIMO-NOMA

The system model assumes a downlink Time division Duplex (TDD) mode based massive MIMO cellular network, as shown in Figure 1

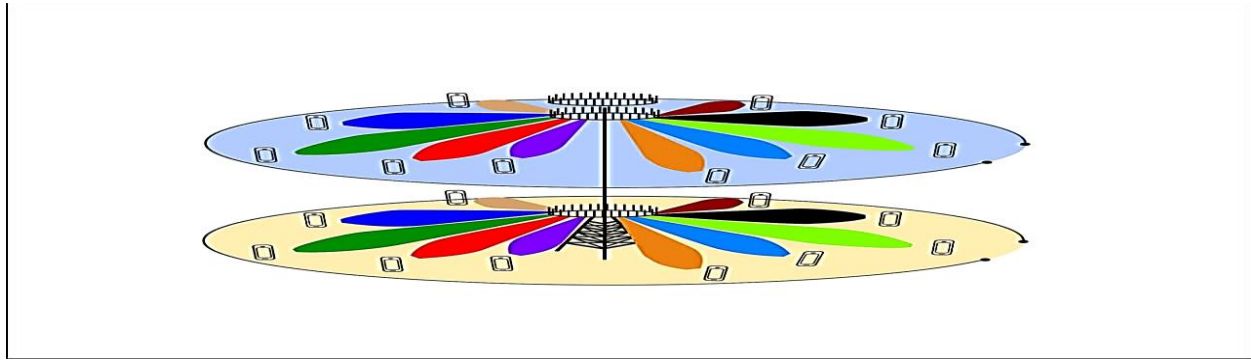


Figure 1: Massive MIMO and Hybrid Precoding

The purpose of beamforming as shown in figure 1 is to amplify transmitted/received signals more in some directions than others to achieve high beamforming gain in the direction of the device of interest to improve link quality in terms of Signal-to-Interference-plus-Noise-Ratio (SINR) and this translates into higher spectral efficiency and/or better coverage for a single link, which in turn results in better network coverage, capacity and user throughput, (David *et.al.*, 2022), (Zelalem *et.al.*, 2022). Figure 1 depicts the implementation of Massive MIMO and Hybrid precoding which is the combination of ZF, MRT and MMSE. The channel is assumed slowly fading and be in the same over the block lengths of the information bearing signals in downlink massive MIMO network, where M -antenna in the BS serve N -single antenna users as shown in Figure 1. The magnitude of M is very large in massive MIMO cellular network for simultaneous data transmission in TDD mode in each coherence time slot. The channel are characterized by both Small Scale Fading (SSF) and Large Scale Fading (LSF) (Tasher *et.al.*, 2019), the k^{th} user's downlink received signal is given as equation 1

$$y_k = G_k X + n_k \quad (1)$$

Where $k = 1, 2, \dots, N$, $G_k \in \mathbb{C}^{M \times 1}$ is the channel gain matrix from M -BS antenna to k^{th} users, the downlink transmitted signal is given in equation 2

$$x = \sum_{i=1}^k \rho_k P_k S_k \quad (2)$$

Where P_k is the k^{th} active user transmitting power scaling factor, ρ_k is the weighed column vector of the beamforming, S_k is the information bearing symbols and $n_k \in \mathbb{C}^{N \times 1}$ is the Additive White Gaussian Noise (AWGN) having identical and independent distribution with zero mean and unit covariance. y_k is the received signal vector by user k .

The channel is assumed to have a known perfect Channel State Information (CSI), linear precoding schemes like ZF, MMSE and MRT are employed in the downlink massive MIMO system to mitigate Inter-User-Interference (IUI) and Inter-Signal-Interference (ISI), with linear precoding, the k^{th} user receiver signal is rewritten in equation 3.

$$y_k = \sqrt{\rho_k} G_k P_k S_k + \sqrt{\rho_k} \sum_{k \in \lambda_{s_i} \neq k} \sqrt{c d_k^{-\ell}} G_k P_i S_i + w_k \quad (3)$$

Where c is LSF factor, d is the distance from k^{th} user to BS antenna, and ℓ is path loss exponent. The respective weighted column vectors of the beamforming codes are shown in equation 4, 5 and 6.

$$P_{ZF} = G^T (G G^T)^{-1} \quad (4)$$

$G = H(H^H H)^{-1}$, H is denoted by the channel matrix containing all users channel

$[h_1, h_2 \dots h_k]$, H^H is the Hermitian matrix of H . G is the channel matrix with the dimension of $M \times K$. (Peerapong *et.al.*, 2018)

$$P_{MMSE} = G^T (G G^T + \Psi_k I_k)^{-1} \quad (5)$$

$$P_{MRT} = G^T \quad (6)$$

Where $\Psi_k = w_k^2 / \rho_k$ denotes the ratio of total noise to transmitting power, $I_k \in \mathbb{C}^{k \times k}$ is the identity matrix of k^{th} column. For equal distribution of power among the users, total transmitting power is given in equation 7

$$P_{total} \geq \sum_{d \in \lambda_s} P d l \quad (7)$$

The k^{th} user received signal as shown in equation 8 – 10 below:

$$y_{k,ZF} = \sqrt{\rho_k} P_{k,ZF} g_k s_k + \sqrt{\rho_k} \sum_{k \in \lambda_s, i \neq k} c d_k^{-\ell} P_{i,ZF} g_k s_i + w_k \quad (8)$$

$$y_{k,ZF} = \sqrt{\rho_k} P_{k,ZF} g_k s_k + \sqrt{\rho_k} \sum_{k \in \lambda_s, i \neq k} c d_k^{-\ell} P_{i,MMSE} g_k s_i + w_k \quad (9)$$

$$y_{k,ZF} = \sqrt{\rho_k} P_{k,ZF} g_k s_k + \sqrt{\rho_k} \sum_{k \in \lambda_s, i \neq k} c d_k^{-\ell} P_{i,MRT} g_k s_i + w_k \quad (10)$$

Where $P_{k,ZF}$, $P_{k,MMSE}$ and $P_{k,MRT}$ are the k th column matrixes of the respective precoding matrix. Optimal distribution of total transmitting power among the users using water-filling algorithm are shown in equation 11 (Shruti *et.al.*, 2022)

$$P_{\lambda_s} = (\delta - \eta)^+ \quad (11)$$

Where $\eta = 1/|g_k^r P|^2$, and $(z)^+$ is the max (0, 2) and δ is water level measured by the equation 11 (Zhe *et.al.*, 2021)

$$P_{total} = \sum_{m \in M} \sum_{k \in N} P_{\lambda_s} \quad (12)$$

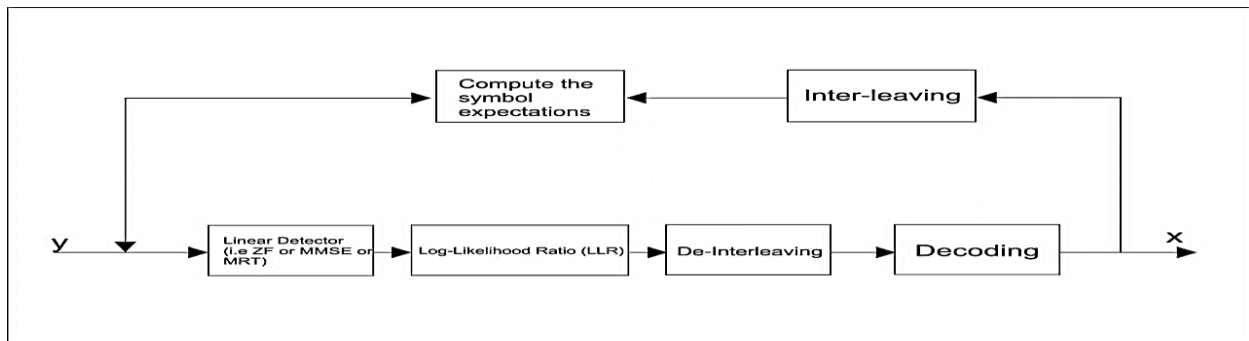


Fig. 2: Example of SIC (Mahmoud *et.al.*, 2019)

As a part of the NOMA transmission protocol, BS utilized superposition coding for the successful transmission of multiple users information simultaneously. It is worth noting that the total power P is distributed equally over all the K UEs. Successive interference cancellation (SIC) is used at the receiver side to extract the information, (Samarendra *et.al.*, 2022). To achieve the system model one need to follow the system algorithm stated in this section.

A wireless cellular network with 10 user equipment is represented as UE (user equipment) in figure 3 and figure 1. Also, figure 3 shows the transmitter side, the channel and the receiver side and explained with equations 14 to 26. The UL NOMA Users, figure 3, at every location of any UE SIC treats detects signals meant for other UE as error through the help of CSI and 128 X 128 massive MIMO systems. In figure 3, U1, U2, U3, U4, U5, U6, U7, U8, U9 and U10 are the ten users with bandwidths 100MHz and $d_1, d_2, d_3, d_4, d_5, d_6, d_7, d_8, d_9$, and d_{10} represent the various BS distances from the respective ten users, $d_1 > d_2 > d_3 > d_4 > d_5 > d_6 > d_7 > d_8 > d_9 > d_{10}$.

Considering the distance, U1 is the weak/far user while U10 is the strong/near user from BS. Let $h_{T_1}, h_{T_2}, h_{T_3}, h_{T_4}, h_{T_5}, h_{T_6}, h_{T_7}, h_{T_8}, h_{T_9}$ and $h_{T_{10}}$ identify which selective Rayleigh fading coefficients they correspond to $|h_{T_1}|^2 < |h_{T_2}|^2 < |h_{T_3}|^2 < |h_{T_4}|^2 < |h_{T_5}|^2 < |h_{T_6}|^2 < |h_{T_7}|^2 < |h_{T_8}|^2 < |h_{T_9}|^2 < |h_{T_{10}}|^2$

2.1.1 For the UL we have

However, in the uplink transmission of NOMA, the signal received at the BS can be expressed as

$$y = \sum_a^A h_a \sqrt{P} x_a + n \quad (13)$$

Where P and x_a are the transmit power and transmit symbols from the a^{th} user, respectively, n refers to AWGN with variance σ^2 , and the number of users sharing the same resource block is A (Rinkoo *et.al.*, 2018). The user's transmit power is limited only by their battery capacity in the uplink, that is all the users can transmit at full strength. Changes in the users' channel gains result to variation in the power domain at the receiver side of BS. Let $x_1, x_2, x_3, x_4, x_5, x_6, x_7, x_8, x_9$ and x_{10} represent the messages that will be sent by ten UL NOMA users U1, U2, U3, U4, U5, U6, U7, U8, U9 and U10 accordingly since $a = 1, 2, 3, 4, 5, 6, 7, 8, 9$ and 10. Assuming the users' signals have the same strength and the network is 128 X 128 massive MIMO system.

Considering the distance, U1 is the weak/far user while U10 is the strong/near user from BS. Let $h_{T_1}, h_{T_2}, h_{T_3}, h_{T_4}, h_{T_5}, h_{T_6}, h_{T_7}, h_{T_8}, h_{T_9}$ and $h_{T_{10}}$ identify which selective Rayleigh fading coefficients they correspond to $|h_{T_1}|^2 < |h_{T_2}|^2 < |h_{T_3}|^2 < |h_{T_4}|^2 < |h_{T_5}|^2 < |h_{T_6}|^2 < |h_{T_7}|^2 < |h_{T_8}|^2 < |h_{T_9}|^2 < |h_{T_{10}}|^2$

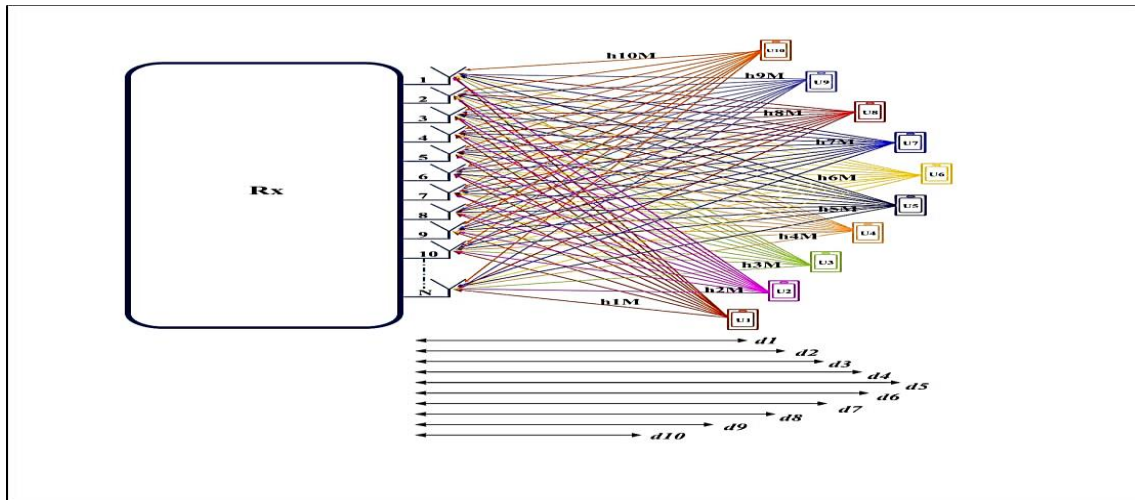


Figure 3: Massive MIMO-NOMA Uplink

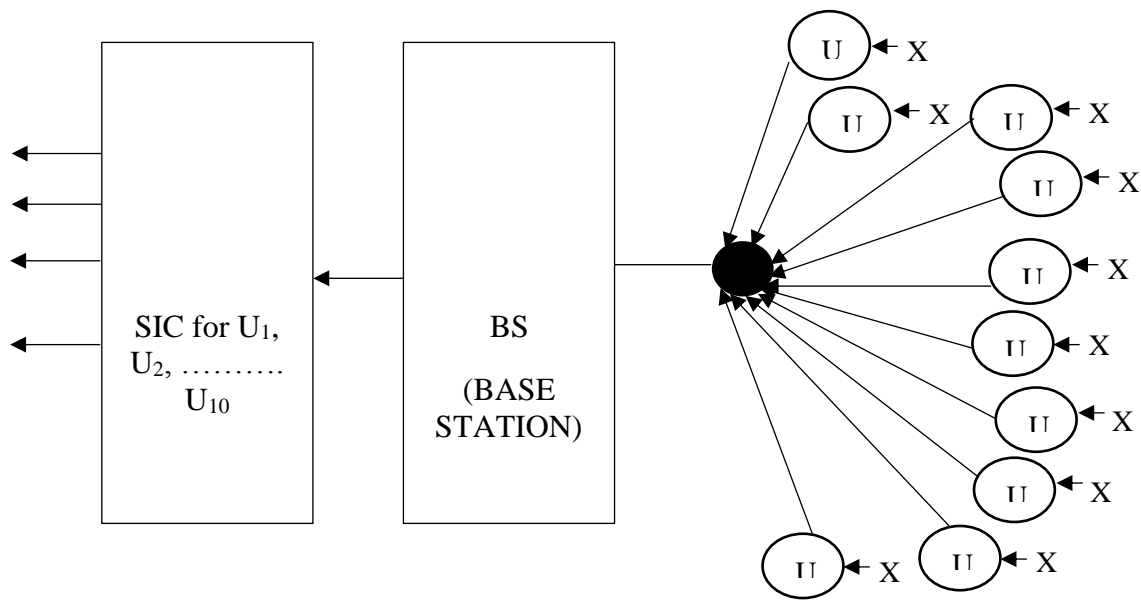


Figure 4: Uplink of Massive MIMO-NOMA system model

The uplink of the system model is represented in figure 4 while Massive the MIMO-NOMA System Model is shown in figure 5

$$h_{jT} = \sum_{j=1}^M h_{jT} \quad (14)$$

Where $j = 1, 2, 3, 4, 5, 6, 7, 8, 9, 10$ ($h_a = h_{jT}$) is the number of users as shown in figure 3, and figure 4, $M = 128$ is the number of channels. $\alpha_1, \alpha_2, \alpha_3, \alpha_4, \alpha_5, \alpha_6, \alpha_7, \alpha_8, \alpha_9$ and α_{10} show their respective power coefficients.

According to the NOMA (power domain) principles, the lower user must have more power (Do *et.al.*, 2020), (Mujtaba *et.al.*, 2022). As a result, the power coefficients must be modified as $\alpha_1 > \alpha_2 > \alpha_3 > \alpha_4 > \alpha_5 > \alpha_6 > \alpha_7 > \alpha_8 > \alpha_9 > \alpha_{10}$ let $x_1, x_2, x_3, x_4, x_5, x_6, x_7, x_8, x_9$ and x_{10} be the QPSK- formed messages to send to BS U1, U2, U3, U4, U5, U6, U7, U8, U9 and U10. The BS's encoded overlay signal is then given by as in Do D. T. *et al.*, (2020).

$$y = \sqrt{P_{x1}h_{1T}} + \sqrt{P_{x2}h_{2T}} + \sqrt{P_{x3}h_{3T}} + \sqrt{P_{x4}h_{4T}} + \sqrt{P_{x5}h_{5T}} + \sqrt{P_{x6}h_{6T}} + \sqrt{P_{x7}h_{7T}} + \sqrt{P_{x8}h_{8T}} + \sqrt{P_{x9}h_{9T}} + \sqrt{P_{x10}h_{10T}} + w \quad (15)$$

Where the noise power is w . Rates Achievable of ten users UL NOMA

The signal from the close user is decoded first, with the signal from the distant users being treated as interference. Therefore, the rate at which the BS can decode the data of a nearby user is given for each user as shown in equations 16 – 25:

$$R_{U10} = \log_2 \left(1 + \frac{P|h_{10T}|^2}{P|h_{1T}|^2 + P|h_{2T}|^2 + P|h_{3T}|^2 + P|h_{4T}|^2 + P|h_{5T}|^2 + P|h_{6T}|^2 + P|h_{7T}|^2 + P|h_{8T}|^2 + P|h_{9T}|^2 + \sigma^2} \right) \quad (16)$$

$$R_{U9} = \log_2 \left(1 + \frac{P|h_{9T}|^2}{P|h_{1T}|^2 + P|h_{2T}|^2 + P|h_{3T}|^2 + P|h_{4T}|^2 + P|h_{5T}|^2 + P|h_{6T}|^2 + P|h_{7T}|^2 + P|h_{8T}|^2 + \sigma^2} \right) \quad (17)$$

$$R_{U8} = \log_2 \left(1 + \frac{P|h_{8T}|^2}{P|h_{1T}|^2 + P|h_{2T}|^2 + P|h_{3T}|^2 + P|h_{4T}|^2 + P|h_{5T}|^2 + P|h_{6T}|^2 + P|h_{7T}|^2 + \sigma^2} \right) \quad (18)$$

$$R_{U7} = \log_2 \left(1 + \frac{P|h_{7T}|^2}{P|h_{1T}|^2 + P|h_{2T}|^2 + P|h_{3T}|^2 + P|h_{4T}|^2 + P|h_{5T}|^2 + P|h_{6T}|^2 + \sigma^2} \right) \quad (19)$$

$$R_{U6} = \log_2 \left(1 + \frac{P|h_{6T}|^2}{P|h_{1T}|^2 + P|h_{2T}|^2 + P|h_{3T}|^2 + P|h_{4T}|^2 + P|h_{5T}|^2 + P|h_{6T}|^2 + \sigma^2} \right) \quad (20)$$

$$R_{U5} = \log_2 \left(1 + \frac{P|h_{5T}|^2}{P|h_{1T}|^2 + P|h_{2T}|^2 + P|h_{3T}|^2 + P|h_{4T}|^2 + \sigma^2} \right) \quad (21)$$

$$R_{U4} = \log_2 \left(1 + \frac{P|h_{4T}|^2}{P|h_{1T}|^2 + P|h_{2T}|^2 + P|h_{3T}|^2 + \sigma^2} \right) \quad (22)$$

$$R_{U3} = \log_2 \left(1 + \frac{P|h_{3T}|^2}{P|h_{1T}|^2 + P|h_{2T}|^2 + \sigma^2} \right) \quad (23)$$

$$R_{U2} = \log_2 \left(1 + \frac{P|h_{2T}|^2}{P|h_{1T}|^2 + \sigma^2} \right) \quad (24)$$

$$R_{U1} = \log_2 \left(1 + \frac{P|h_{1T}|^2}{\sigma^2} \right) \quad (25)$$

These equations define the intrinsic features of the Massive MIMO-NOMA concept in this work and the mathematical analysis obtained with the system model, was used in obtaining a better result as shown figure 5.

5G and Beyond needs massive MIMO-NOMA in order to offer reliable QoS, massive connectivity, very high spectrum efficiency and lower latency. MATLAB codes was used to develop a massive MIMO-NOMA wireless network whose internal subsystems were analyzed, MATLAB codes were also used to validate the influence of massive MIMO-NOMA in 5G wireless network. The achieved a very high spectrum efficiency at the uplink as shown in figure 6. Figure 7, massive MIMO-NOMA system model was implemented using MATLAB codes and simulation parameters in table 1.

2.1.2 Massive MIMO-NOMA Simulation Parameters

The parameters specified in Table 1 were used for running and deriving simulation results from 100 simulations seed templates.

In the simulation scripts for Massive MIMO-NOMA, via the simulation model template, The model based on Table 1, allows for the investigation of network reliability with Massive MIMO-NOMA system by plotting graphs of spectral efficiency against transmit power and other selected metrics to show an enhance optimal Massive MIMO-NOMA network with massive connectivity.

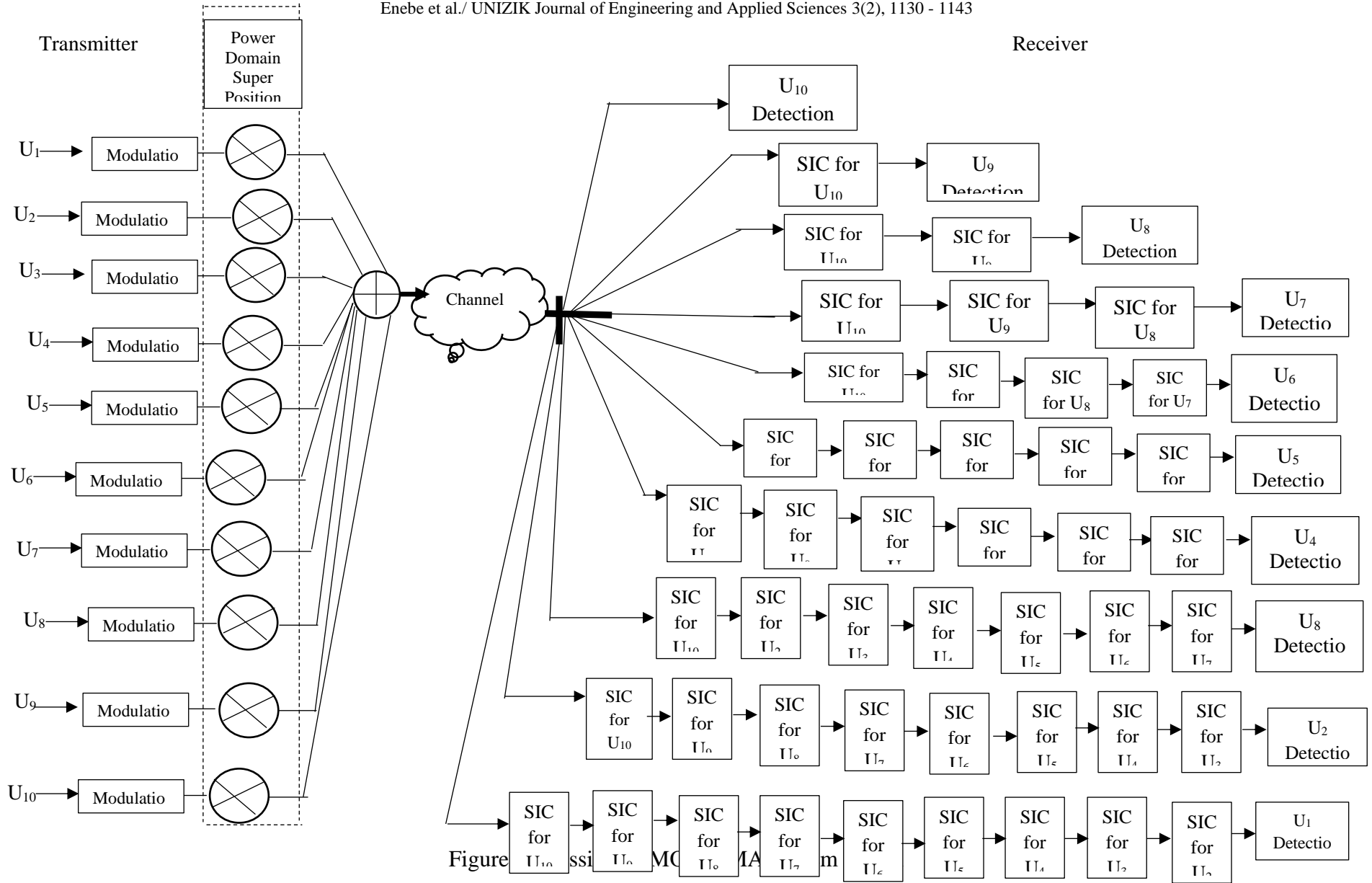
Essentially, to enhance spectral efficiency of 5G network, Massive MIMO-NOMA was employed. In the simulation scenario, massive MIMO antenna was used by implementing beamforming, precoding, user scheduling, channel estimation and signal detection.

2.2 System Algorithm

The system algorithm was developed in order to establish the step by step structural organization of the Massive MIMO-NOMA, considering the attenuation and fading of the network from 10m to 100m.

Table 1: Implementation Parameters (Source: Testbed field parameters (MTN Nigeria), MATLAB, 2022)

Parameter	Specifications
Number of users	10
Frequency band	N78 (3.5GHz)
Max. Transmission power	240mW (23.8dBm)
Cell Radius	5000
Bs-2-Bs Distance	7500
Massive MIMO	128 X 128
Path loss Exponent	4
Antenna Height	22m
Modulation	QPSK
Bandwidth (BW)	100MHz
Number of Simulations	1000
Power Coefficient	Monte Carlo simulation
Fading Coefficient	Monte Carlo simulation



3.0 Results and Discussions

The goal of this paper is to improve and reassess the spectrum efficiency (SE) of the uplink (UL), best capacity rate in a 5G network using Massive MIMO-NOMA. The proposed model utilizes QPSK modulation, 10 users with different power location coefficients, SNR, transmit power, and bandwidths 100 MHz under selective frequency Rayleigh fading channels

Each figure should have a caption as shown in figure 1. The caption should be concise and typed separately, not on the figure area. Figures should be self-explanatory. Information presented in the figure should not be repeated in the table. All symbols and abbreviations used in the illustrations should be defined clearly. Figure legends should be given below the figures

Spectrum Efficiency vs Transmitting Power at 100MHz BW with Massive MIMO-NOM.

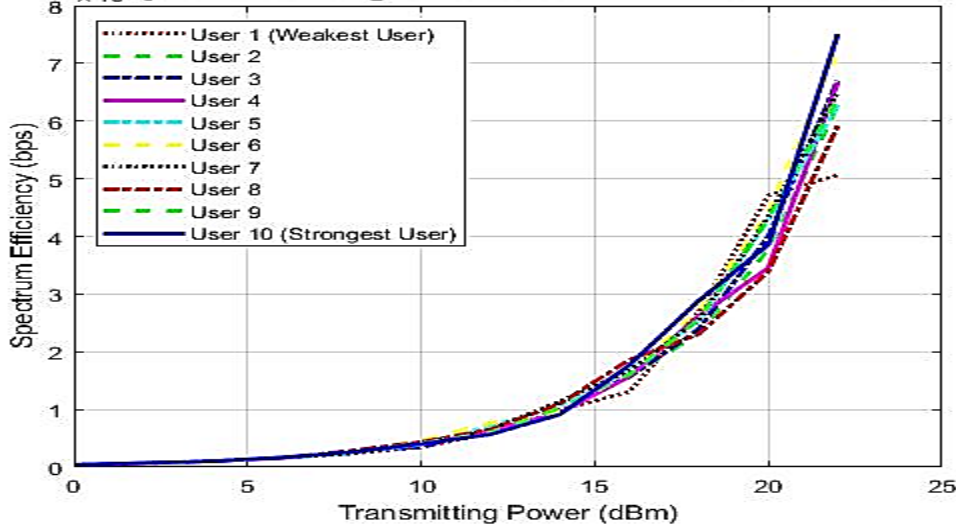


Figure 6: Spectrum Efficiency against Transmitting Power

Figure 6: shows the result from UL of massive MIMO-NOMA of Spectrum Efficiency against Transmitting Power. At Transmitting power of 10dBm all the users appeared to be one and had spectrum efficiency of 4021.48bps. At Transmitting power of 20dBm the users with the least spectrum efficiency are user4 and user8 with spectrum efficiency of 33905.4bps while the best performing user is user1 (the weakest user) with spectrum efficiency of 47090.3bps, showing 27.99% better than user4 and user8 which are 40m and 80m away from the base station respectively while user1 is 100m away from the base station. The result shows that far-near problem is completely eliminated by massive MIMO-NOMA scheme while observing the spectrum efficiency increase as Transmitting power increases.

Also the strongest user (user10), positioned 10m away from the base station has spectrum efficiency of 38575.3bps when compared with the weakest user, user1 at transmitting power 20dBm outperformed the strongest user, (user10) by 18%. Also when compared with the result of spectrum efficiency against SNR in Shiguo *et.al.*, (2021), 96% improvement was recorded. Generally, because of the implementation of SIC at the uplink of massive MIMO-NOMA all the users were the impact of changing the transmission power level on spectral efficiency of the uplink.

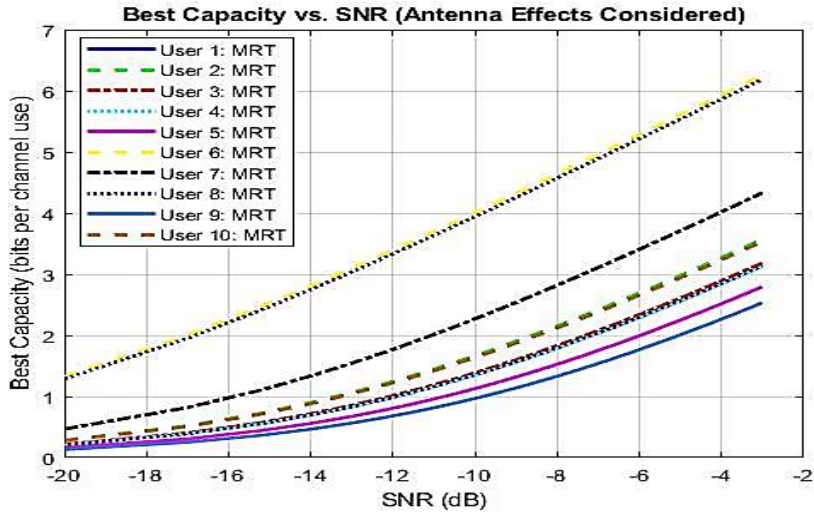


Figure 7: Best Capacity against SNR when MRT was selected as the precoding technique of the massive MIMO-NOMA network.

At lower SNR the MRT is selected over ZF and MMSE, figure 7 showed that the proximity of the user to base station does not determine the performance of the user in terms best capacity. The best performing users are user6 and user8 with best capacity of 5.83499 bits per channel use, while the strongest user (user10) in terms of proximity to the base station had best capacity of 3.20801 bits per channel use, showing that user6 and user8 outperformed user10 by 45% in terms of best capacity.

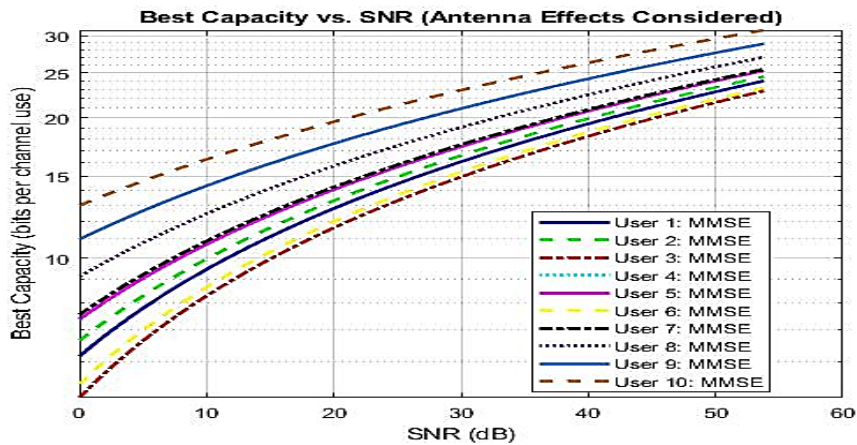


Figure 8: Best Capacity against SNR when MMSE precoding technique was selected in the massive MIMO-NOMA network.

Figure 8 show result of Best capacity against SNR when MMSE is selected over MRT and ZF. At very high SNR, MMSE is selected over MRT and ZF. It is observed that due to the effect of MMSE on the network the users did not perform exactly according to its proximity to the base station, in one instance at 20dB of SNR user1 out performed user6 by 6%. As best capacity was increasing, SNR was also increasing and each time the simulation was run, the users recorded different result. In some cases, high best capacity was recorded while in some cases low best capacity was recorded. Figure 9 shows the result of BER against transmitting power for ten users massive MIMO-NOMA.

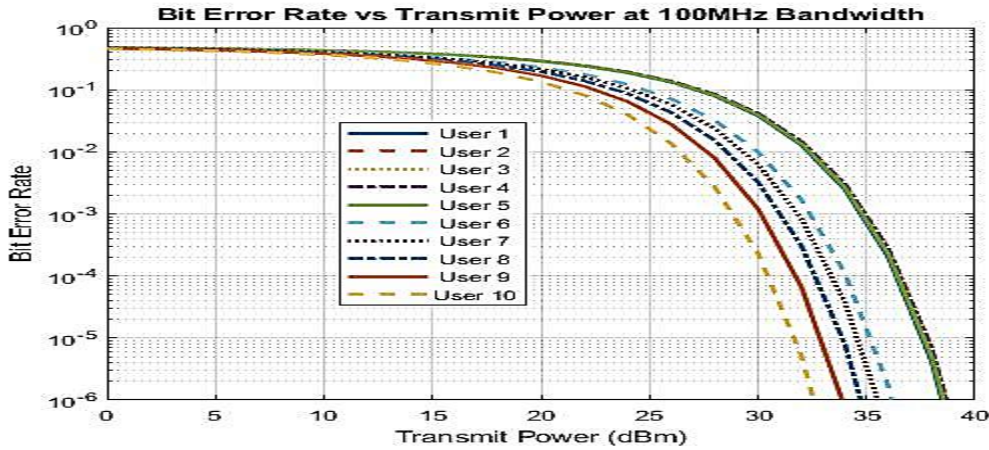


Figure 9: Bit Error Rate against Transmit Power

Figure 9 shows that for weakest user (user1) the optimal massive MIMO-NOMA has BER of 5.02002×10^{-6} at Transmitting power of 38dBm with bandwidth of 100MHz while in Mohamed *et al* (2022) at transmitting power of 38dBm with bandwidth of 200MHz the strongest users (user4) had a BER of 46×10^{-4} , the optimal massive MIMO-NOMA showed 99% reduction in BER when compared with result of Mohamed *et al*, (2022). Both the users were 100m away from the base station. Figure 10 is graph of spectral efficiency against SNR for 10 users massive MIMO-NOMA with 256-QAM modulation.

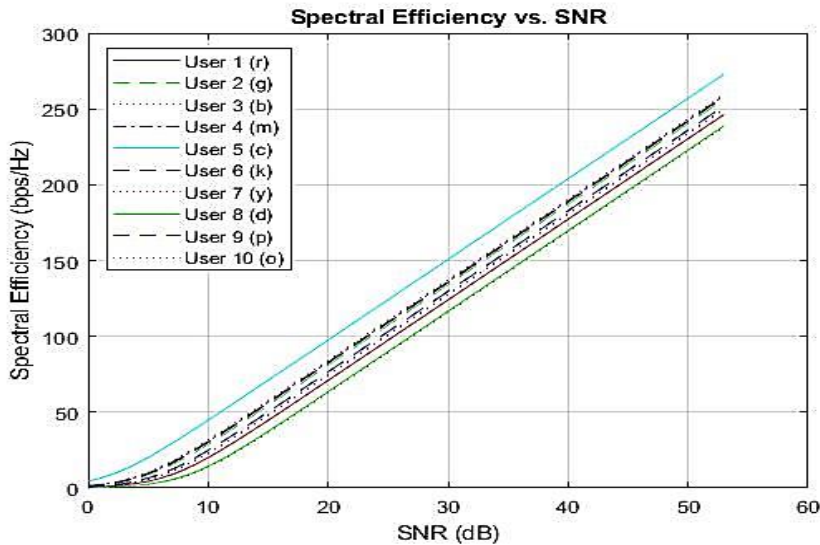


Figure 10: Spectral Efficiency against SNR (dB)

Figure 10 shows that as SNR increases, spectral efficiency also increases. User5 achieved the highest spectral efficiency of 43.2674bps/Hz while User2 had the least spectral efficiency of 20.3993bps/Hz at 10dB of SNR. Comparing the result of best performing user, that is user5, with the result from Samarendra *et.al.*, 2022, the proposed model achieved 85.46% improvement in spectral efficiency.

4.0. Conclusion

This paper meticulously examined and demonstrated the improvement of uplink spectral efficiency of 5G network using Massive MIMO-NOMA. Ten user Non-orthogonal Multiple Access Power Domain (NOMA PD) was modelled and developed to achieve optimal result when combined with massive MIMO that utilizes ZF-MRT-

MMSE hybrid precoder. The results showed that the incorporation of ten users NOMA into massive MIMO network yielded the best performance in terms of uplink spectral efficiency per users, bit error rate when compared to other strategies used by previous authors. Among the diverse dimensions of 5G and beyond, the integration of Massive MIMO and Non-Orthogonal Multiple Access (NOMA) emerges as a remarkable technique. Massive MIMO-NOMA effectively addresses the need for enhanced spectral efficiency yielding a network with higher data rate, enhanced Connectivity and coverage and support for diverse applications. By allowing multiple users to share the same frequency and time resources simultaneously, Massive MIMO-NOMA optimizes network performance.

Conclusively, using massive MIMO-NOMA to improving the uplink spectral efficiency of 5G network is essential for realization of the full potential of 5G technology and delivering high-performance and reliable wireless connectivity to users around the world. These are obviously important as the demand for wireless connectivity continues to grow, and sustainability becomes a key consideration for network operators and regulators.

References

- Antonio, A and Jacek I, 2024. A Survey of NOMA-Aided Cell-Free Massive MIMO Systems. *Electronics* 2024, 13, 231. <https://doi.org/10.3390/electronics13010231>, Received: 1 December 2023, Revised: 26 December 2023 Accepted: 27 December 2023, Published: 4 January 2024
- Arthur, S. S., Francisco R. M. L., Daniel B. C., Zhiguo D., Pedro H. J., Nardelli, U. S. D., Constantinos B. P., 2020. Massive MIMO-NOMA Networks with Imperfect SIC: Design and Fairness Enhancement. *IEEE Transactions on Wireless Communications*, Volume 19, issue 9, Pp. 6100 – 6115, September 2020.
- Dang, X. T., Hieu V. N., and Oh-Soon S., 2023. Optimization of IRS-NOMA-Assisted Cell-Free Massive MIMO Systems Using Deep Reinforcement Learning, Received 13 June 2023, accepted 18 August 2023, date of publication 30 August 2023, date of current version 7 September 2023. Digital Object Identifier 10.1109/ACCESS.2023.3310283
- David A., Peter V. B., Sebastian F., Erik L., 2022. Meeting 5G network requirements with Massive MIMO. *Ericsson Technology Review*, February 16, 2022.
- Do, D. T., Nguyen, T. L., Ekin, S., Kaleem, Z., Voznak, M. 2020. Joint user grouping and decoding order in uplink/downlink MISO/SIMO-NOMA. *IEEE Access* **2020**, 8, 143632–143643. [CrossRef]
- Chen, C., Zhong, W. D. Yang, H. and Du, P., 2018. On the Performance of MIMO-NOMA-Based Visible Light Communication Systems, in *IEEE Photonics Technology Letters*, vol. 30, no. 4, pp. 307-310, 15 Feb.15, 2018, doi: 10.1109/LPT.2017.2785964.
- Hien, Q. Ngo., 2020. 5G and Beyond: Fundamentals and Standards, Massive, MIMO. Book Chapter, Pp 101 – 127, 12 August 2020, Xingqin Lin Namyoon Lee Editors.
- Linglong, D., Bichai, W., and Zhiguo, D., 2018. A Survey of Non-Orthogonal Multiple Access for 5G. *IEEE Communications Surveys & Tutorials*, Vol. 20, No. 3, Third Quarter 2018
- Mahmoud, A. A., Markku J., and Shahriar S., 2019. Massive MIMO Detection Techniques: A Survey. *JOURNAL OF LATEX CLASS FILES, VOL. 14, NO. 8, AUGUST 2019*
- Mahmoud, A. A., Alaa, A., Ammar, M. A., and Salama, I., 2021. Overview of Precoding Techniques for Massive MIMO. 10.1109/ACCESS.2021.3073325, *IEEE Access*
- Mahmoud A. A., Kumar A, A., Khan I, Choi B. J., 2020. Comparative analysis of data detection techniques for 5G massive mimo systems. *Sustain* 2020;12:1–12. <https://doi.org/10.3390/su12219281>.
- Mahmoud A. A. M., Salah W., Kumar A., Alsharif M. H., Rambe A. H., Jusoh, M., 2021. Low Complexity Linear Detectors for Massive MIMO: A Comparative Study. *IEEE Access* Received March 1, 2021, accepted March 10, 2021, date of publication March 15, 2021, date of current version March 29, 2021. *Digital Object Identifier 10.1109/ACCESS.2021.3065923*

- Mohammed, E., and Mahmoud A. A., 2022. Low Complexity Linear Detectors for Massive MIMO with Several Antenna Array Configurations: A Comparative Study. *International Journal of Electrical and Electronic Engineering & Telecommunications*, received February 13, 2022; revised April 3, 2022; accepted May 11, 2022.
- Mohamed, H., Manwinder, S., Khalid, H., Rashid, S., Maha, A., Raed, A., and Nidhal, O., 2023 Enhancing NOMA's Spectrum Efficiency in a 5G Network through Cooperative Spectrum Sharing. *Electronics* 2023, 12, 815. <https://doi.org/10.3390/electronics12040815>, Received: 14 January 2023, Revised: 31 January 2023, Accepted: 3 February 2023, Published: 6 February 2023.
- Mohamed, H., Manwinder, S., Khalid, H., Rashid, S., Maha, A., and Raed, A., 2022. Modeling of NOMA-MIMO-Based Power Domain for 5G Network under Selective Rayleigh Fading Channels. *Energies* 2022, 15, 5668. <https://doi.org/10.3390/en15155668>, Received: 12 July 2022, Accepted: 1 August 2022, Published: 4 August 2022
- Mujtaba, G., Ahmad, K. H., Ziaul, H. A., Ghulam, A., Aseel, H., and Thar, B., 2022. Cooperative Power-Domain NOMA Systems: An Overview. *Sensors* 2022, 22, 9652. <https://doi.org/10.3390/s22249652>, Received: 30 September 2022, Accepted: 3 December 2022, Published: 9 December 2022
- Peerapong, U., Arfat, A. K., Monthippa, U., and Pumin, D., 2018. Energy Efficient Design of Massive MIMO Based on Closely Spaced Antennas: Mutual Coupling Effect energies, Received: 10 July 2018; Accepted: 2 August 2018; Published: 5 August 2018.
- Rajpreet, S., Paras, C., 2020. Hybrid Beamforming for millimetre Wave massive MIMO Communication: A Survey. *International Journal of Advance Science and Technology* Vol. 29, No. 10S, (2020), pp. 1888-1897 ISSN: 2005-4238 IJAST 1888
- Rao, M., A., Mustafa, S., Ateeq, Ur R. , Muhammad, S., Rehan, A. K., and Wali, U. K., 2022. Performance Evaluation of Spectral Efficiency for Uplink and Downlink Multi-Cell Massive MIMO Systems. *Hindawi Journal of Sensors*, Volume 2022, Article ID 7205687, 12 pages, <https://doi.org/10.1155/2022/7205687>.
- Ridho, H., Yoga, P., Toan-Van, N., Yushintia, P., Kyusung, S., and Beongku A., 2023. *International Conference on Artificial Intelligence in Information and Communication (ICAIIIC) | 978-1-6654-5645-6/23 ©2023 IEEE | DOI: 10.1109/ICAIIIC57133.2023.10067078*
- Rinkoo, B., 2018. Multiple Access Techniques For 5g Networks. *International Journal Of Engineering Technologies And Management Research, Vol.5 (Iss.2: SE): February, 2018* [*Communication, Integrated Networks & Signal Processing-CINSP 2018*] ISSN: 2454-1907 DOI: 10.29121/ijetmr.v5.i2.2018.661.
- Robin, C., Robert A., 2020. An Efficient and Fair Scheduling for Downlink 5G Massive MIMO Systems. Accepted at Texas Symposium on Wireless and Microwave Circuits and Systems, IEEE 2020, Conference Paper · March 2020 DOI: 10.1109/WMCS49442.2020.9172382, <https://www.researchgate.net/publication/339663733>
- Robin, C., and Robert A., 2020. Massive MIMO Systems for 5G and beyond Networks Overview, Recent Trends, Challenges, and Future Research Direction. *Sensors* 2020, 20, 2753, Received: 9 April 2020; Accepted: 7 May 2020; Published: 12 May 2020, www.mdpi.com/journal/sensors
- Robin, C., and Robert A., 2019. Channel Gain Based User Scheduling for 5G Massive MIMO Systems. Accepted at The 16th International Conference on Smart Cities: Improving Quality of Life Using ICT & IoT and AI, IEEE HONET-ICT 2019, See discussions, stats, and author profiles for this publication at: <https://www.researchgate.net/publication/337509047>
- Samarendra, N. S., D, Kandar, A. S., Nhan, D. N., Sukumar, N., and Dinh-Thuan, D., 2022. Hybrid Precoding Algorithm for Millimeter-Wave Massive MIMO-NOMA Systems. 2022
- Senel, K., Hei, V. C., 2019. Emil Bjornson and Ehat Role Can NOMA Play in Massive MIMO, *Journal of Selected Topics in Signal Processing*, Feb. 2019

- Shiguo, W., Youan, L., Rukhsana, R., Xuewen, F., 2021. Clustering and power optimization in mmWave massive MIMO–NOMA systems. Contents lists available at Science Direct, Physical Communication 49 (2021) 101469 journal homepage: www.elsevier.com/locate/phycom
- Shruti, R., Danve1, M. S., Nagmode, S. Deosarkar, B., 2022. Transmit Antenna Selection in Massive MIMO: An Energy-Efficient Approach. International Journal of Engineering Trends and Technology Volume 70 Issue 12, 170-178, December 2022 ISSN: 2231 – 5381 / <https://doi.org/10.14445/22315381/IJETT-V70I12P218>
© 2022 Seventh Sense Research Group
- Tasher, A. S., Joyatri, B., Md.Anwar, H., 2019. Capacity maximizing in massive MIMO with linear precoding for SSF and LSF channel with perfect CSI. Science Direct Digital Communications and Networks journal homepage: [www. https://doi.org/10.1016/j.dcan.2019.08.002](http://www.https://doi.org/10.1016/j.dcan.2019.08.002) Received 26 January 2019; Received in revised form 19 June 2019; Accepted 29 August 2019 Available online 4 September 2019 2352-8648/© 2019 Chongqing University of Posts and Telecommunications. Publishing Services by Elsevier B.V. on behalf of KeAi Communications Co. Ltd.
- Zelalem, M. G., Ram, S. S., Satyasis, M., and Davinder, S. R., 2022. Efficient Hybrid Iterative Method for Signal Detection in Massive MIMO Uplink System over AWGN Channel. Hindawi Journal of Engineering Volume 2022, Article ID 3060464, 19 pages <https://doi.org/10.1155/2022/3060464>
- Zhe, L., Sahil, V., and Machao, J., 2021. Power Allocation in Massive MIMO-HWSN Based on the Water-Filling Algorithm. Hindawi Wireless Communications and Mobile Computing Volume 2021, Article ID 8719066, 11 pages <https://doi.org/10.1155/2021/8719066>, Received 30 April 2021; Revised 1 June 2021; Accepted 10 July 2021; Published 10 August 2021